

## S3-8-3

## CHARACTERIZATION OF PORTLAND CEMENT PASTE USING MIP, NANOINDENTATION AND ESEM TECHNIQUES

Richard J. AQUINO

*PhD student, Materials & Environment, Microlab, Delft University of Technology, Delft, The Netherlands*

Dessislava A. KOLEVA

*Assistant Prof., Materials & Environment, Microlab, Delft University of Technology, Delft, The Netherlands*

Eduard A.B. KOENDERS

*Associate Prof., Materials & Environment, Microlab, Delft University of Technology, Delft, The Netherlands and Visiting Prof., COPPE/UF RJ, Programa de Engenharia Civil, Rio de Janeiro, Brasil*

Klaas VAN BREUGEL

*Professor, Materials & Environment, Microlab, Delft University of Technology, Delft, The Netherlands*

### ABSTRACT:

The performance of concrete is increasingly designed through durability. Durable concrete is a driving force for a sustainable production and use of cement. One way to achieve durability of concrete is to fathom the mechanical properties of the cement matrix and the main associated features of its microstructure. Non-destructive experimental methods such as nanoindentation and ESEM were used to characterize the hardened Portland cement paste with  $w/c=0.40$  hydrated at 7, 14 and 28 days. Grid indentation analysis was employed between approximately two equal sized hydrated cement particles. Additionally, MIP was used as a generally accepted technique for deriving porosity and pore size distribution and results correlated to those received from ESEM image analysis.

**Keywords:** cement microstructure, characterization, nanoindentation, ESEM, performance, sustainability

### 1. INTRODUCTION

The performance of concrete is increasingly designed through durability. Durable concrete is a driving force for a sustainable production and use of cement, i.e. the main binder of concrete. Concrete is a composite material in which the hardened cement paste acts as the main binder that “holds everything together”. Thus, the properties of this binder are critical to the performance of concrete as a whole. The engineering properties of cement and concrete are known to be porosity dependent, and characterization of the pore system is often a better predictor of performance than characterization of the solid phases [1].

One way to achieve durability of concrete is to fathom the mechanical properties of the cement matrix and the main associated features of its microstructure, i.e. total porosity, pore size distributions, permeability, phase volume distribution, etc. Hence, the goal of this study is to characterize the hardened Portland cement (CEM I 42.5N) paste using a combination of well accepted and more sophisticated techniques, e.g. Mercury intrusion porosimetry (MIP), nanoindentation and mathematical morphology and stereology approach for image analysis of cement-based microstructure, based on micrographs, captured with environmental scanning electron microscope (ESEM). The results will be used for the validation of a conceptual model developed as part of the CODICE project

([www.codice-project.eu](http://www.codice-project.eu)). The model is expected to quantify the potential microstructural growth of hydration products and addresses the link between the micro- to nano- level models as developed in CODICE.

### 2. EXPERIMENTAL PROCEDURES

#### 2.1 Material and sample preparation

The material used in this study was ordinary Portland cement (CEM I 42.5N). Cement paste of  $w/c = 0.4$  was prepared by mixing with an electric mixer for 5 min. After mixing, the cement pastes were cast into a plastic cylindrical container and sealed. Mixing and storage took place at room temperature; curing (hydration) ages were 7, 14 and 28 days. At each specified curing period, samples of thickness around 5 mm were produced from each relevant cement paste cylinder, by cutting the latter in the middle. Cement hydration was ceased through submersion in liquid nitrogen, followed by vacuum freeze-drying (for water removal through sublimation) until constant sample weight was achieved. For image analysis based on ESEM micrographs, the samples were further subjected to vacuum-impregnation with epoxy resin and oven-dried for 24 h to harden the epoxy resin while the samples for nanoindentation and energy-dispersive x-ray spectroscopy (EDX) analysis were not subjected to any epoxy impregnation. All samples followed well known procedures for sample preparation of grinding, using a

series of silicone carbide paper of increasing (fineness) mesh sizes 500, 800, 1200 and 4000 followed by polishing using diamond particles of sizes 6, 3, 1 and 0.25  $\mu\text{m}$ . Ethanol was used during grinding and polishing of the specimens to prevent further hydration of the paste due to eventual water penetration. Finally, the polished specimens were cleaned in an ultrasonic-bath for 5 min to remove debris possibly embedded in pores during the process of grinding and polishing.

## 2.2 Characterization techniques

### (1) Mercury intrusion porosimetry

MIP is widely used technique in measuring porosity-related characteristics of a porous material. MIP tests were conducted by using Micromeritics Poresizer 9320 (with a maximum pressure of 207 MPa) to determine the porosity and the pore size distribution of the specimens. In this method, the dried porous sample i.e. the hardened cement paste is placed into a chamber, the chamber is evacuated, and mercury is added inside the chamber, then an external pressure is applied on the mercury. As the pressure gradually increases, mercury is forced into the pores of the cement paste. The applied pressure,  $P$  (MPa) is inversely proportional to the size of the pores as defined by Washburn equation [2],

$$d = -4\gamma \cdot \cos(\varphi) / P \quad (1)$$

where,

$d$  : apparent pore diameter ( $m$ )

$\gamma$  : mercury surface tension ( $N/m$ )

$\varphi$  : contact angle between mercury and pore wall

During the MIP test, two sample replicates were used for each hydration period to ensure repeatability of the experiment.

### (2) Image analysis

The backscattered electron (BSE) mode of the ESEM was used to obtain a grey-scale BSE images. The combination of BSE images and quantitative image analysis allows deriving structural information of pore space, such as porosity and critical pore size. On the basis of mathematical morphology transformations, pore size distribution can be obtained by using a sequence of similarly shaped structuring elements of increasing size [3].

The original (or selected area of) BSE image is segmented by applying a grey-level threshold to create a binary image, reflecting the pore phase [3,4]. The binary image is then subjected to quantitative image analysis for derivation of structural parameters, i.e. pore size distribution, critical pore size, pore connectivity, etc. The “opening distribution” technique was used, whereby the binary image is opened by a series of squares of increasing size [3,5]. The cumulative pore size distribution curve is obtained by plotting the pore area fraction after an opening operation versus linear

dimension of the structuring element. This gives a type of “size” classification in the case of an interconnected structure, like pore space in concrete. The critical pore size,  $l_c$  can be conceived as the diameter of the pore that completes the first interconnected pore pathway in a network, developed by a procedure of sequentially adding pores of diminishing size to this network. The critical pore size is a unique transport length scale of major significance for permeability properties and can be associated with the inflection point of the cumulative pore size distribution curve.

### (3) Nanoindentation

The used of nanoindentation to measure the elastic properties of hydrated cement pastes is relatively recent technique, providing a lot of opportunities to characterize the material at micro- to nano- level [6]. Nanoindentation tests were conducted using Agilent Nano Indenter G200 to determine the elastic modulus  $E$  of different phases (e.g. unhydrated cement particles and C-S-H). The local mechanical properties can be determined from indentation load and displacement measurement. Information on the micro-mechanical properties was obtained from a matrix of a minimum of 120 indents covering a representative area of at least  $40 \times 230 \mu\text{m}^2$  on the surface. The selected indent spacing was 10  $\mu\text{m}$ . The indentation depth performed was 200 nm within the range that allows access to the in situ properties of C--S--H, CH, and unhydrated cement phase [7]. A Berkovich tip was used for the indentation. The continuous stiffness method (CSM method) developed by Oliver and Pharr [8] was used for the analyses of the results and the average  $E$ -modulus was determined in the loading range between 100 and 180 nm depths. At continuous changes of penetration depth,  $h$  of the indenter the applied load,  $F$  is uniformly increasing/decreasing is monitored. A typical example of an indentation curve is shown in Fig. 1. Using a con-

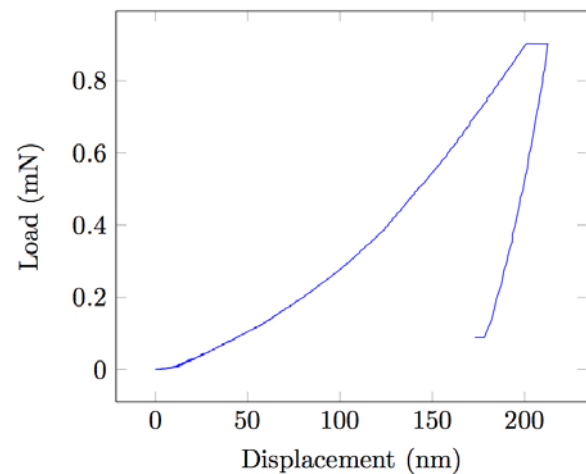


Fig. 1 Typical indentation load-depth hysteresis curve taken during one indentation

tinuum scale model, the indentation hardness,  $H$  and modulus,  $E_m$  are determined using the following formulas,

$$H = F_{max} / A_c \quad (2)$$

$$S = dF / dh_{max} = 2\beta \cdot E_m (A_c / \pi)^{0.5} \quad (3)$$

where  $\beta$  is a dimensionless correction factor and all the quantities required to determine  $H$  and  $E_m$  can be obtained directly from the  $F-h$  curve except the contact area,  $A_c$  that can be extrapolated from the maximum depth,  $h_{max}$ . Assuming an isotropic case, the problem is reduced to a plane-stress elastic modulus

$$E_m = E / (1-\nu^2) \quad (4)$$

where,

$E_m$  : indentation modulus

$E$  : elastic modulus

$\nu$  : Poisson's ratio of the indented material

#### (4) ESEM

Philips XL30 ESEM with EDX was used during the entire experiment. The ESEM is equipped with different types of imaging detectors such as the secondary electrons (SE) and backscattered electrons (BSE) imaging. The BSE imaging is a grey-scale detector with the brightness directly proportional to the average atomic number of the material. Thus, the region that appears bright has a high average atomic number compared to those dark regions with lower average atomic values.

Aside from the spatial resolution capability, the ESEM can also be extended to qualitative and quantitative chemical analysis of specimens using the EDX detector. The EDX was calibrated using standard materials before any chemical analysis to ensure accurate chemical measurements.

### 3. RESULTS AND DISCUSSIONS

#### 3.1 MIP test

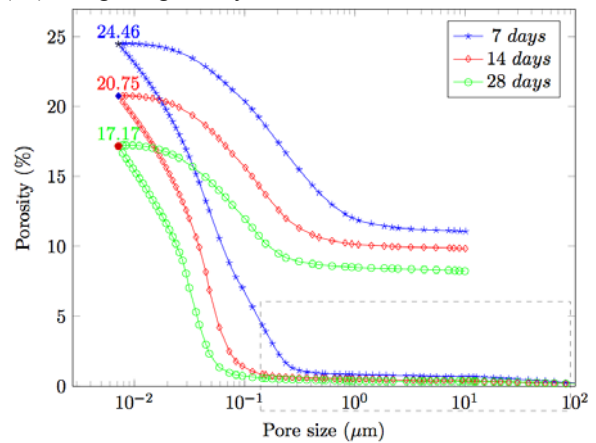
The characterization of the pore structure of cement paste using MIP is important in understanding the mechanical and transport properties of cement paste. In MIP testing, the porosity is measured by entering a progressive volume of mercury using external pressure into the (dried) pore system. The intruded volume of mercury is then plotted as a function of the external pressure that gives an indication of pore size distribution, i.e. how the total porosity is distributed among different pore sizes.

At time zero, the space originally occupied by water comprises the capillary porosity (as well as the pore size distribution) that decreases with hydration time. Fig. 2 shows the porosity and pore size distribution of hardened Portland cement pastes as measured by MIP technique using a water-cement ratio of 0.40 and hydrated at 7, 14 and 28 days. As expected, the porosity and pore size distribution decreased as hydration continues.

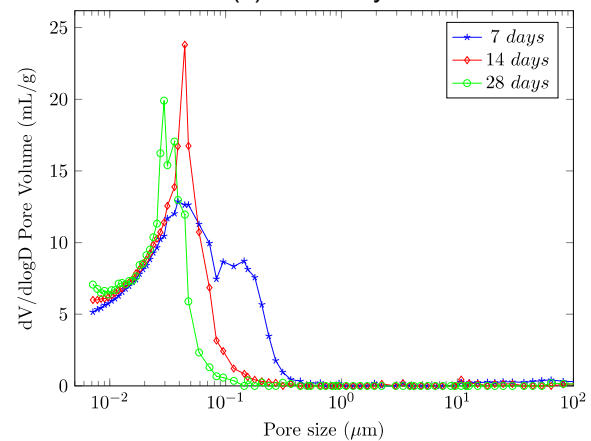
#### 3.2 Microstructural analysis

The microstructural investigations were conducted

using ESEM in BSE mode, operating at an accelerating voltage of 20 kV for imaging. For each hydration ages, an average of 20 images per sample of 15x15 mm<sup>2</sup> for the bulk matrix in each specimen were recorded. The images were taken at magnification of 500x where the physical size of the reference region of each image is 226  $\mu$ m in length and 154  $\mu$ m in width giving a resolution of 0.317  $\mu$ m/pixel. The image analysis (IA) was performed using OPTIMAS software package and based on mathematical morphology and stereology approach [3,5]. The results are as expected, there is a reduction of the porosity, critical pore size and permeability with time of cement hydration. Fig. 3 depicts the derived porosity (3a) and critical pore size (3b) using image analysis.



(a) Porosity

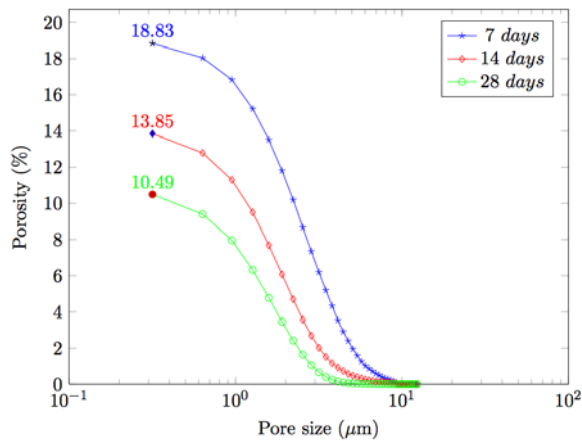


(b) Critical pore size

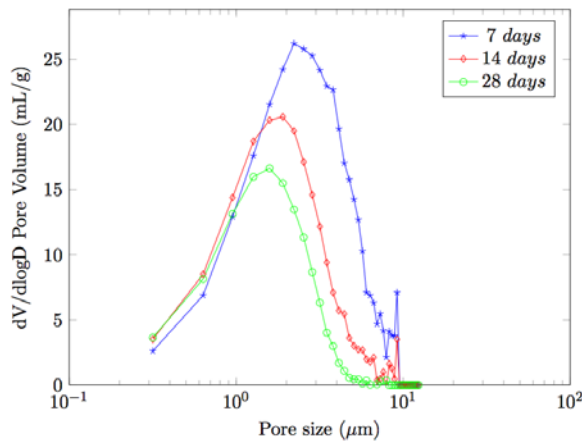
Fig. 2 The porosity (a) and critical pore size (b) of hardened cement paste (CEM I 42.5N) with w/c = 0.40 hydrated at 7, 14 and 28 days measured using Mercury intrusion porosimetry.

A direct absolute comparison of values derived from MIP and image analysis is not possible and would be inaccurate. As abovementioned, conventional techniques, as MIP, also result in indicative values. Therefore, absolute values are not claimed neither for MIP nor image analysis results. What is important for the purpose of microstructural investigation is comparing and evaluating the trends of change in porosity and pore size distribution of equally handled samples, which as seen from Figs. 2 and 3 is similar for

both techniques and is as expected within the process of cement hydration. For all hydration ages of 7, 14 and 28 days, the MIP results present analogical trend of material behaviour as subsequently defined within image analysis for these time intervals (the rectangular area in Fig. 2a defines the region, where image analysis can determine porosity and pore size). What should be also noted is that averaging all data, derived from image analysis, will lead to inaccurate results. Therefore systematical sampling strategy was used in order to obtain the final values. Fig. 4 shows a comparison of the capillary porosity using computer simulation and as measured by MIP and IA.



(a) Porosity



(b) Critical pore size

Fig. 3 The porosity (a) and critical pore size (b) of hardened cement paste (CEM I 42.5N) with w/c=0.4 hydrated at 7, 14 and 28 days analyzed using image analysis.

The distribution of phases and pore connectivity were calculated as well. Fig. 5 presents summarized data for the phase distribution (including porosity values) per hydration stage. The main reaction products of tricalcium silicate (C<sub>3</sub>S) (main ingredient of Portland cement) and water are calcium silicate hydrate (C-S-H) and calcium hydroxide (CH). The hydration products expand around 2.2 times the volume of hydrated C<sub>3</sub>S. This explains why the porosity is reduced during hydration since C-S-H and CH occupies more space. Also, the unhydrated cement (UC) naturally decreases

within the process of cement hydration i.e. with the formation of hydration products.

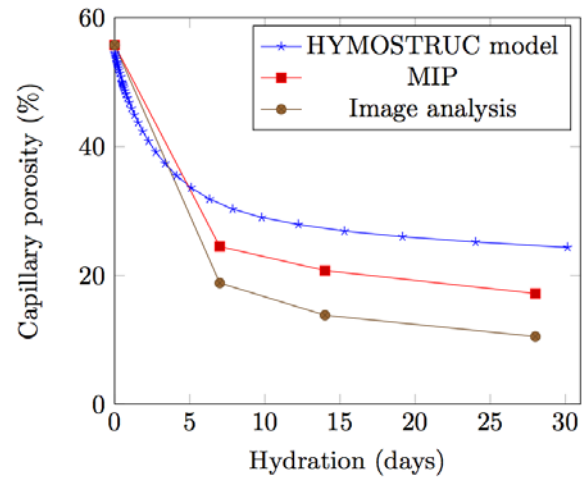


Fig. 4 The porosity of hardened cement paste (CEM I 42.5N) with w/c=0.4 hydrated at 7, 14 and 28 days as determined by MIP and IA including values derived from HYMOSTRUC-3D model [9].

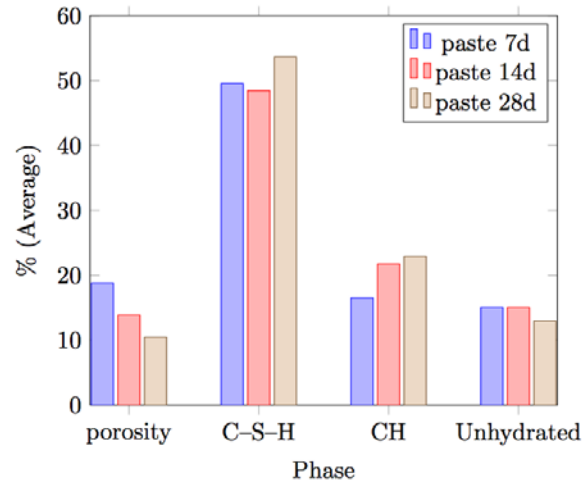


Fig. 5 Phase distribution of hardened cement paste using w/c=0.4 per hydration stage of 7, 14 and 28 days, i.e. porosity, C-S-H, CH and unhydrated cement derived from IA.

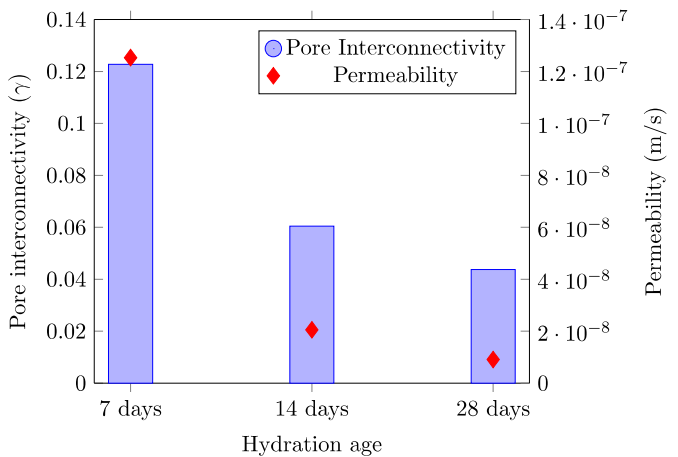


Fig. 6 Pore connectivity and permeability of the cement matrix with w/c=0.4 hydrated for 7, 14 and 28 days derived from IA.

Fig. 6 shows the calculated pore connectivity and permeability of the cement matrix hydrated for 7, 14 and 28 days. Both parameters are reduced during hydration. The importance of the permeability of cement paste is related to penetration and transport of aggressive substances e.g. Cl, CO<sub>2</sub> into the bulk cement-based matrix.

### 3.3 Nanoindentation

The grid-indentation technique was employed to study in detail the two adjacent hydrated cement particles that include UC, C-S-H, CH, pores and other hydration products. The two neighboring hydrated cement particles were first chosen with the aid of the ESEM before any nanoindentation measurement was done. The spacing between indents was set to 10- $\mu\text{m}$  in both perpendicular directions and the number of indents along the x-axis and y-axis was chosen based on the distance between cement particles. The Poisson's ratio was assumed using a value of 0.18. The indentation was chosen between two  $\sim 40 \times 40 \mu\text{m}$  diameter cement particles at a distance of around 2-3 times the particle diameter. Fig. 7a depicts the original BSE image of the

cement paste at 28 days of age, showing in particular the region between two cement grains, where nanoindentation was performed i.e. modulus of elasticity was recorded and the corresponding bulk density was derived. The relevant mapping results are depicted in Figs. 7b and 7c. The modulus of elasticity was a direct result of nanoindentation. The C-S-H density was calculated using the equation developed by a group in Tecnalia [10] as a function of the modulus of elasticity of C-S-H, express as

$$E_{CSH} = 78.88\rho_{CSH} - 123.47 \quad (5)$$

where,

$$E_{CSH} : \text{C-S-H modulus of elasticity (GPa)}$$

$$\rho_{CSH} : \text{C-S-H density (g/cm}^3\text{)}$$

The different phases according to  $E$  used in different contour interval and the corresponding densities of Fig. 7 are shown in Table 1. The C-S-H are usually classified as low density (LD), high density (HD) and ultra-high density (UHD).

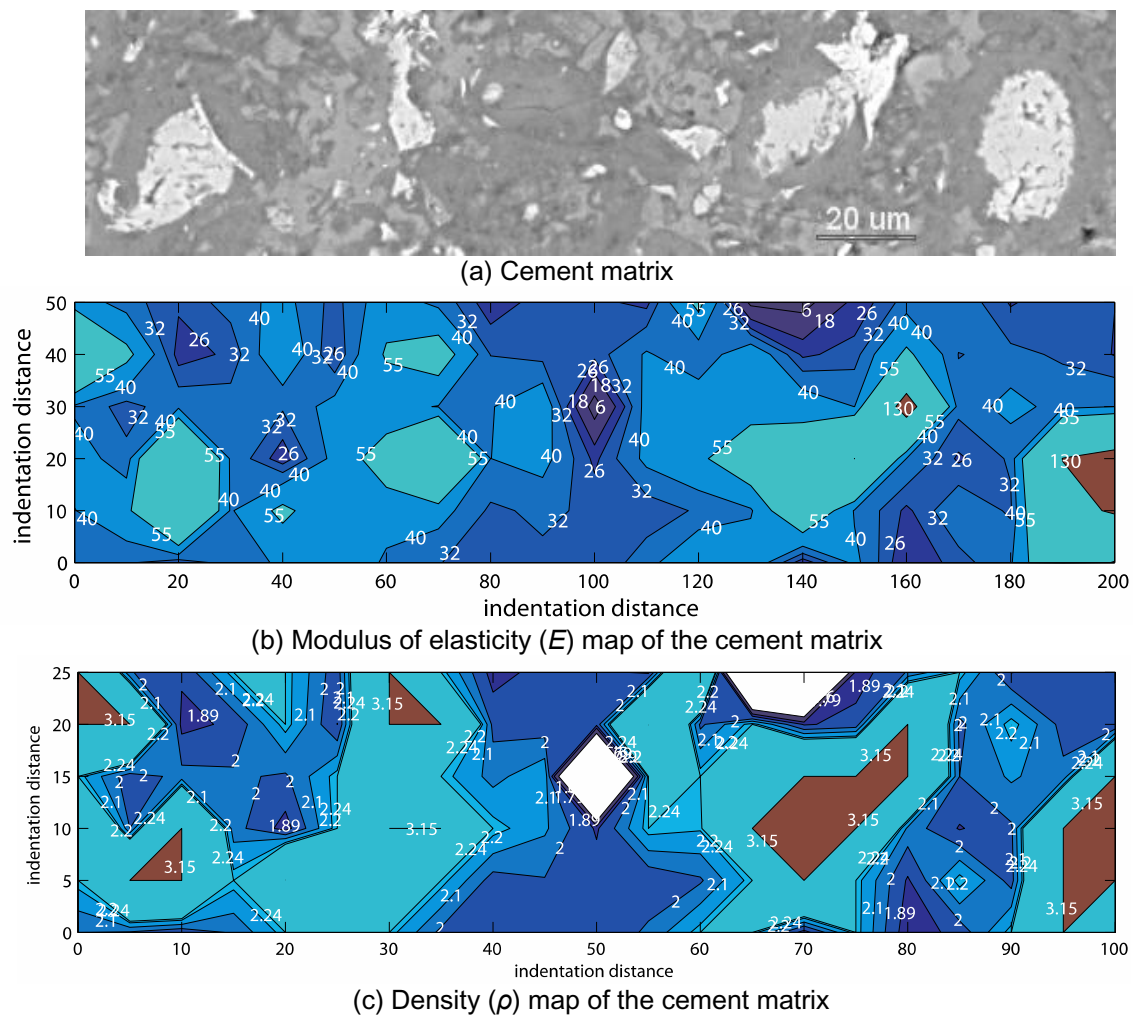


Fig. 7 Mapping of modulus of elasticity and density of the cement matrix ( $w/c=0.4$ ) hydrated at 28 days between two adjacent hydrated cement particles of sizes  $\sim 40 \times 40 \mu\text{m}$  at a distance approximately 2-3 times the particle diameter. Note that indentation distance is 10  $\mu\text{m}$  apart. The density of both C<sub>3</sub>S and CH were assumed to be equal to 3.15 and 2.24 g/cm<sup>3</sup> [11], respectively.

Table 1. Phase classifications according to  $E$  in GPa (as adapted from [12] with few modifications) used in different contour intervals and the corresponding densities in  $\text{g/cm}^3$  used in this paper.

Phases	$E$	Dry density
Pores/Low stiffness C-S-H	0-18	-
LD C-S-H	18-26	1.79-1.89 <sup>a</sup>
HD C-S-H	26-35	1.89-2.01 <sup>a</sup>
UHD C-S-H	40-45	2.07-2.14 <sup>a</sup>
CH	33-44	2.24 [11]
Unhydrated	45-160	3.15 [11]

<sup>a</sup>The range of values as computed using the measured  $E$  based on eqn. (5).

## 5. CONCLUSIONS

The characterization of hardened Portland cement paste is of fundamental importance in understanding the mechanical and transport properties of cementitious materials. The hardened cement paste is the main binding material of concrete. Porosity is one of the intrinsic characteristics of cement paste and as such determines long-term performance in terms of microstructural and mechanical properties. It is therefore of great importance to accurately determine microstructural characteristics, especially if a modeling approach to defining transport and hydration mechanisms is foreseen. A combination of conventional and more sophisticated techniques was hereby used to determine microstructural characteristics of cement paste, aiming to aid the on-going numerical simulation. The main conclusions are summarized as follows:

- (1) As expected porosity, critical pore size, pore interconnectivity, permeability and unhydrated cement decrease with hydration time.
- (2) The amount of reaction products such as C-S-H and CH increase as hydration continues.
- (3) Image analysis captures the general trends of porosity and critical pore size development of cement paste as also measured by MIP.
- (4) Nanoindentation as a non-destructive method is indispensable in determining the elastic properties of the microstructure. The C-S-H density can be determined by linear relationship of the C-S-H modulus of elasticity.

## ACKNOWLEDGEMENT

This work was supported by the Seventh Framework Program theme 4 NMP of the European Commission under the Computationally Driven design of Innovative Cement-based materials (CODICE) project ([www.codice-project.eu](http://www.codice-project.eu)) under grant agreement no. 214030. Also, the main author would like to thank Arjan Thijssen for the assistance in using the ESEM/EDX and performing the MIP experiment. Further, Dr. Oguzhan Copuroglu is acknowledged for helpful discussion for the main author to understand and perform the full quantitative chemical analysis and for analyzing the results. In addition, the authors are grateful to Prof. dr. ir. Erik Schlangen in helping to carry-out the nanoindentation experiments.

## REFERENCES

1. Thomas, J. and Jennings, H., "A monograph – The Science of Concrete", <http://iti.northwestern.edu/>, accessed June 12, 2012.
2. E.W. Washburn, The dynamics of capillary flow, *Phys. Rev.* 17 (3) (1921) 273–283.
3. Hu, J., "Porosity of Concrete – Morphological Study of Model Concrete." Phd thesis, 2004.
4. Ye, G., "Experimental study and numerical simulation of the development of the microstructure and permeability of cementitious materials." Phd thesis, 2003.
5. Hu, J. and Stroeven, P., "Application of image analysis to assessing critical pore size for permeability prediction of cement paste," *Image Analysis Stereology*, Vol. 22, 2003, pp.97-103.
6. Constantinides, G., Chandran, K.S.R., Ulm, F.J. and van Vliet, K.J., "Grid indentation analysis of composite microstructure and mechanics: Principle and validation", *Materials Science and Engineering A*, Vol. 430(1-2), 2006, pp.189-202.
7. Constantinides, G. and Ulm, F. J., "The nanogranular nature of C-S-H", *Journal of the Mechanics and Physics of Solids*, Vol. 55 (1) 64-90.
8. W.C. Oliver and G.M. Pharr, Measurement of hardness and elastic modulus by instrumented indentation: advances in understanding and refinements to methodology, *J. Mater. Res.* 19 (1) (2004) 3–20.
9. van Breugel, K., "Simulation of hydration and formation of structure in hardening cement-based materials." Phd thesis, 1997.
10. Tecnalia, <http://www.labein.es/>, accessed 2011.
11. Taylor, H. F. W., "Cement Chemistry", London, Thomas Telford, 1997.
12. Zhu, W., et al., "Nanoindentation mapping of mechanical properties of cement paste and natural rocks", *Materials Characterization*, Vol. 58(11-12), 2007, pp. 1189-1198.